
Papers

Radiation flux balance of the sea–atmosphere system over the southern Baltic Sea*

OCEANOLOGIA, 40 (4), 1998.
pp. 277–306.

© 1998, by Institute of
Oceanology PAS.

KEYWORDS

Solar radiation
Sea surface radiation
Radiation flux balance
Southern Baltic

SŁAWOMIR KACZMAREK,
JERZY DERA
Institute of Oceanology,
Polish Academy of Sciences,
Powstańców Warszawy 55, 81–712 Sopot, Poland; e-mail: kaczmar@iopan.gda.pl

Manuscript received September 28, 1998, in final form November 9, 1998.

Abstract

Developed at IO PAS, Sopot, and first presented at the BALTEX Study Conference in Visby (Dera *et al.*, 1995), the improved radiation transfer model was applied to determine the following radiation fluxes in the southern Baltic region: the flux entering the Earth's atmosphere Q_1 , the sum of fluxes absorbed Q_2 and scattered upwards (reflected) in the atmosphere $Q_{2'}$, the direct solar ray flux reaching the sea surface Q_3 , the diffuse solar flux (scattered downwards in the atmosphere) reaching the sea surface Q_4 , the total solar flux reaching the sea surface Q_5 , the total flux reflected by the sea surface Q_6 , the total flux entering the water column Q_7 , the flux scattered upwards by the water body and leaving the sea surface Q_8 , the flux absorbed in the water column Q_9 , that absorbed by the water itself Q_{10} , that absorbed by admixtures other than phytoplankton pigments Q_{11} , and that absorbed by phytoplankton pigments Q_{12} , the photosynthetically stored radiation flux Q_{13} and the effective infrared radiation flux at the sea surface Q_{14} .

The model has been developed for the application of satellite images as the main source of input data. However, since the relevant satellite data are not yet

* This work was carried out within the framework of the BALTEX Programme and was financially supported by the Polish State Committee for Scientific Research.

The major part of the paper was presented at the Second Study Conference on BALTEX, Juliusruh, Rügen, Germany, 25–29 May 1998.

available, a long-term meteorological and bio-optical standard database has been used in the computations. The mean monthly fluxes and their balances for the southern Baltic region, divided into 20 sub-regions, have been obtained for each month of the year.

1. Introduction

The fluxes of radiant energy flowing through the atmosphere, penetrating the usually wave-roughened sea surface and entering the water column in the sea, exert a decisive influence on numerous dynamic, thermodynamic, chemical and biological processes occurring in the sea-atmosphere system. These fluxes are therefore fundamental components of the energy balance of the marine environment and, for application in diverse meteorological, hydrological and climatological models, have to be accurately determined. Furthermore, in studies and the modelling of the ecologically and biologically significant cycles of carbon and other essential elements, it is important to know the quantities of solar energy available to all levels of the biosphere. The last ten years have witnessed the development of numerous techniques for utilising the laws of radiation transfer through the atmosphere and sea in the remote sensing of a variety of environmental properties and processes, such as the chlorophyll concentration and the rate of primary production of organic matter in the sea. For these and other reasons, a very large number of papers deal with the study and modelling of radiant energy transfer through the atmosphere and sea (see *e.g.* Timofeyev, 1983; Lenoble, 1985; Trenberth, 1992 and Mobley, 1994). In most of them the problems of cloudless and cloudy skies have been addressed separately. The models applicable to cloudless skies generally make use of simplified forms of the radiative transfer equation (*e.g.* Bird and Riordan, 1986; Green *et al.*, 1988; Gueymard, 1993). On the other hand, the effect of cloudiness on the transmission of light energy is accounted for by empirical relationships derived for given weather conditions, types of cloud cover and geographical regions. Reviews of such models can be found in Timofeyev (1983), and Dobson and Smith (1988). The inaccuracies in these methods of determining the mean annual energy fluxes reaching the sea surface can be far in excess of 10 W m^{-2} (Dobson and Smith, 1988).

The problems of radiant energy transfer in the sea-atmosphere system in the context of remote sensing are discussed in depth by Raschke (1996). Pomeranec (1966) carried out a penetrating study of the complete energy balance of the Baltic, in which the heat balance model was based on some 70 thousand empirical hydrometeorological data from the period 1867 to 1955 and the actinometric data available at the time of writing. Czyszek *et al.* (1979), Krężel (1985) and Dera and Rozwadowska

(1991) elaborated further models and statistical relationships of solar energy fluxes reaching the surface of the Baltic. These workers established successive approximations of the mean monthly solar energy totals and approximate formulas for calculating them on the basis of long-term hydrometeorological and actinometric data obtained from Baltic shore stations and the available optical data from Baltic research cruises. However, these were non-spectral data and models, precluding high precision. In striving for a more accurate description of the energy reaching the Baltic, the first spectral model of solar radiation transmission through the atmosphere over the Baltic was developed (Woźniak and Rozwadowska, 1995), and soon afterwards, a spectral model of the transfer of this radiation across a real, *i.e.* wave-roughened and foam-covered, sea surface (Woźniak S. B., 1996a,b, 1997) was conceived. At the same time, the numerous underwater hydro-optical studies carried out in the past decade have borne fruit in the form of optical and bio-optical models of the water column (Morel, 1988, 1991; Woźniak and Pelevin, 1991; Woźniak *et al.*, 1992, 1997). The application of these latest models to the case two waters of the Baltic (Kaczmarek and Woźniak, 1995) enabled the computations to be performed which are presented in the present paper. The bio-optical model of the water column is perhaps the most accurate aspect of the model (see the review by Dera, 1995).

The aim of the present paper is to compute, with the aid of the coupling spectral model, the set of 14 components of the radiant energy flux that are the principal components of the energy balance of the atmosphere and the Baltic Sea. Because most of the available empirical input data (Augustyn, 1985) were given as monthly means for 20 sub-regions of the southern Baltic, the present description will be restricted to the mean monthly values of these fluxes there. The 'classical' method of estimation (Gulev, 1997) is applied in which monthly mean values of the hydrometeorological data are taken as input data to the model.

2. Materials and methods

The fourteen fundamental radiant energy fluxes usually distinguished in the sea-atmosphere system have been determined in this paper (Fig. 1). They are: the flux entering the Earth's atmosphere Q_1 , the sum of fluxes absorbed Q_2 and scattered upwards (reflected) in the atmosphere $Q_{2'}$, the direct solar ray flux reaching the sea surface Q_3 , the diffuse solar flux (scattered downwards in the atmosphere) reaching the sea surface Q_4 , the total solar flux reaching the sea surface Q_5 , the total flux reflected by the sea surface Q_6 , the total flux entering the water column Q_7 , the flux scattered upwards by the water body and leaving the sea surface Q_8 , the flux absorbed

in the water column Q_9 , that absorbed by the water itself Q_{10} , that absorbed by admixtures other than phytoplankton pigments Q_{11} , and that absorbed by phytoplankton pigments Q_{12} , the photosynthetically stored radiation flux Q_{13} and the effective infrared radiation flux at the sea surface Q_{14} .

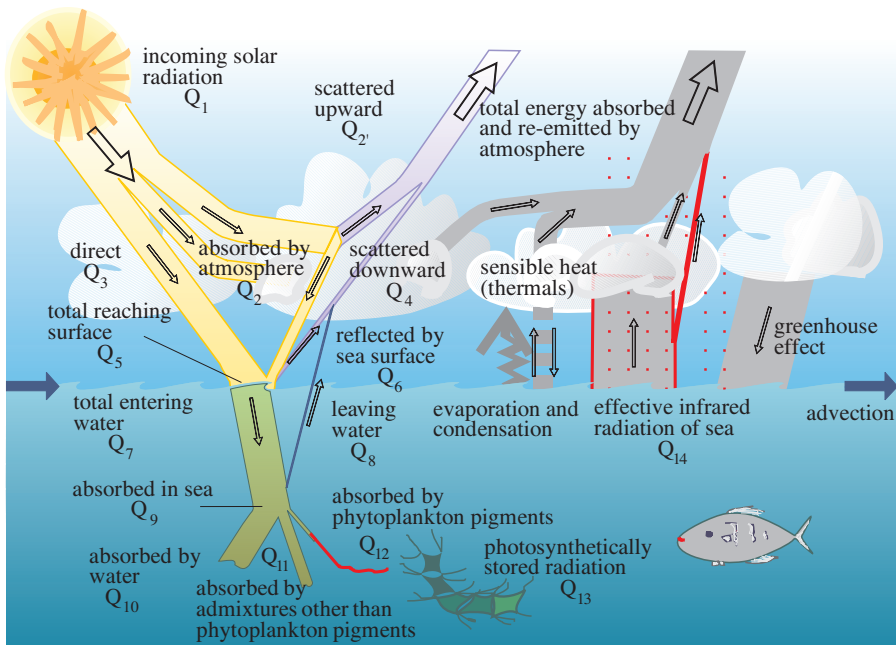


Fig. 1. Principal energy fluxes in the atmosphere–ocean system (adapted from Trenberth, 1992, by A. Rozwadowska)

The subscript numbers attached to the fluxes above and in Fig. 1 serve to identify them in the tables, figures and text.

The model used in the computations can be presented in the form of a block diagram (Fig. 2). This consists of blocks of input data, model formulae allowing the desired quantities to be computed, and computed flux magnitudes. The model formulae have been divided into five modules: the equation of the geometry of the Sun–Earth system, the atmospheric optical transmittance model, the sea–surface optical transmittance model, the water bio-optical model, and formulae for the effective surface infrared radiation.

Three of the models mentioned above have been developed for the Baltic region by the optical group at IO PAS Sopot over many years of investigations, and have been described in numerous papers: the atmospheric spectral optical model, still in its initial stages, (Woźniak and Rozwadowska, 1995);

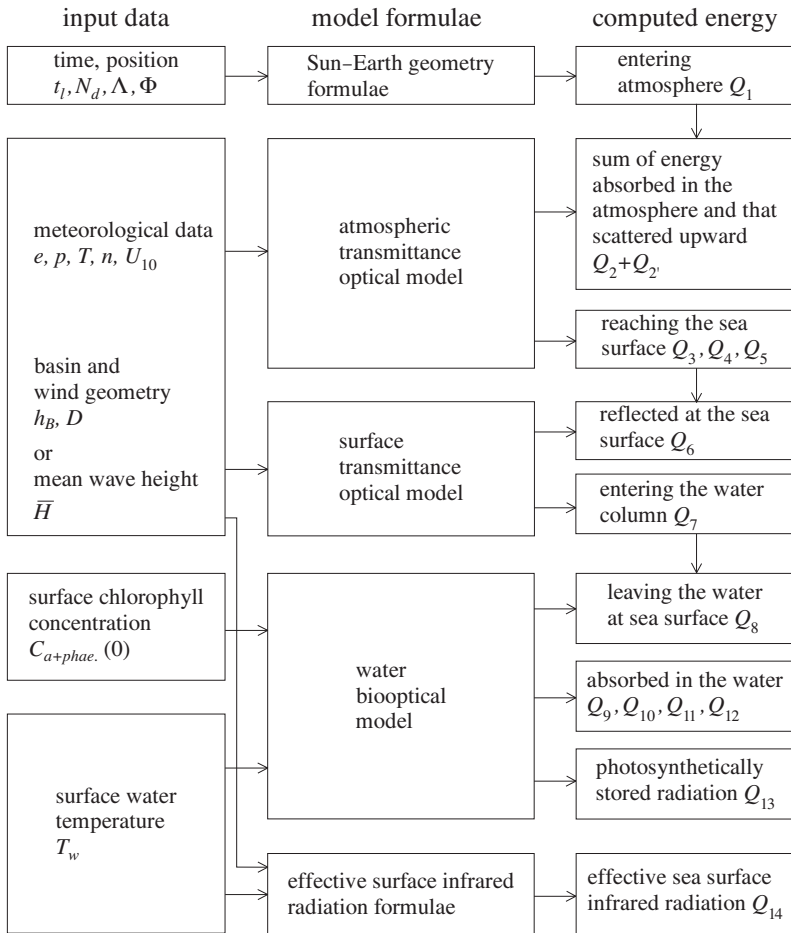


Fig. 2. Block diagram of the algorithm for computing energy fluxes

the spectral optical model of sea surface transmittance (Woźniak S.B., 1996a,b, 1997); the spectral bio-optical model of the Baltic water column (Kaczmarek and Woźniak, 1995), based on an earlier model for oceanic waters (Woźniak *et al.*, 1992). The algorithm itself is described in detail in Woźniak *et al.* (in press).

The formula for the effective infrared radiation through the sea surface was adopted from Bignami *et al.* (1995). Based as it is on a very large quantity of carefully measured, marine, empirical data this formula seems to be the most appropriate of those currently available:

$$\begin{aligned}
 Q_{14} &= IR \uparrow - IR \downarrow = \\
 &= \varepsilon \sigma T_w^4 - \left[\sigma T_p^4 (0.653 + 0.00535 e_1) \right] \times (1 + 0.1762 n_8^2), \quad (1)
 \end{aligned}$$

where

$IR \uparrow$ – upward radiation flux emitted by the sea,

$IR \downarrow$ – downward radiation flux emitted by the atmosphere to the sea,

$\varepsilon = 0.98$ – water emittance,

$\sigma = 5.6697 \times 10^{-8} \text{ W m}^{-2} \text{ K}^{-4}$ – Stefan-Boltzmann constant,

e_1 – water vapour pressure [mb],

n_8 – total cloud cover [range 0–8].

The following quantities serve as the input data of our complex model:

n – total cloud cover [range 0–1],

p – atmospheric pressure [hPa],

T_a – surface air temperature [$^{\circ}\text{C}$],

e – relative air humidity over the sea surface [range 0–1],

\bar{H} – mean height of wind waves [m],

U_{10} – wind speed at standard level 10 m [m s^{-1}], also wind direction,

D – wind fetch [m],

h_B – depth of the basin [m],

$C_a(0)$ – surface concentration of chlorophyll a [mg m^{-3}],

$T_w(0)$ – sea surface temperature SST [$^{\circ}\text{C}$].

To determine the solar zenith angle Θ , time and geographical position are necessary:

t_l – local solar time,

N_d – number of the day in the year,

Λ – latitude,

Φ – longitude.

The mean diurnal magnitude of each flux in each month of the year was calculated. The input data were the mean monthly values of the above quantities, determined from long-term figures for each of the sub-regions on the modelling grid (roughly for the period 1970–1990). With the exception of the Sun's daily path, the diurnal variability of the separate parameters was not taken into consideration. The Sun's daily path was accounted for by repeating the calculations for successive solar altitudes at 30-minute intervals, the other values being kept constant, and integrating the results.

Both the time intervals and the subdivision of the study area (see the model grid – Fig. 3) applied in this work were determined solely by the available empirical input data. The model itself, including all three of its principal components, *i.e.* for the atmosphere, sea surface and water column, does not impose any such limitations in the Baltic region beyond the area of water covered by ice.

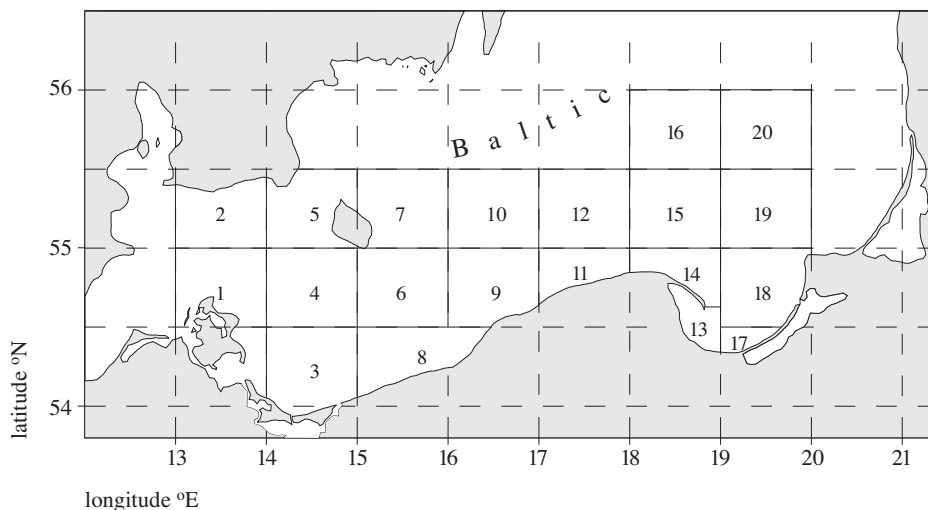


Fig. 3. The study area with numbered sub-regions

Most of the input data for the model were taken from publications of the Institute of Meteorology and Water Management (Augustyn, 1985), where the multi-annual monthly means of the hydrometeorological parameters for the grid in Fig. 3 are calculated. The spatial and temporal distributions of the surface concentrations of chlorophyll *a* were established for this grid from our own data obtained from the IO PAS data bank¹, and from the data kindly made available to us by the Sea Fisheries Institute, Gdynia, and to a small extent by HELCOM (in all, around 1700 readings).

At the same time, the parameters of the model equations applied to specific local conditions and for verifying the computation results were determined from the available empirical data on the following quantities:

- $E_d(0^-, \lambda)$ – downward spectral irradiance at the sea surface (0^- signifies ‘in air’) [$\text{W m}^{-2} \text{ nm}^{-1}$],
- $E_d(0^-, \text{total})$ – downward irradiance at the sea surface in the total spectral range of solar radiation [W m^{-2}],
- $E_d(0^-, \text{PAR})$ – downward irradiance at the sea surface for the PAR spectral range (Photosynthetically Available Radiation) [W m^{-2}],
- $R(0^-, \lambda)$ – spectra of the reflectance function at the sea surface (ratio of upward to downward irradiance),
- $K_d(z, \lambda)$ – vertical and spectral distributions of the downward irradiance diffuse attenuation function [m^{-1}],

¹Regional Oceanographic Database of IO PAS: www/iopan.gda.pl/rbdo/index.html

- $C_a(z)$ – vertical distribution of chlorophyll *a* + *phae.* concentration [mg m⁻³],
 $P(z)$ – vertical distribution of primary production in the sea [mgC m⁻³ day⁻¹],
 $a_{pl}(z, \lambda)$ – vertical and spectral distribution of the light absorption coefficient of phytoplankton pigments [m⁻¹].

Data on these quantities were gleaned from a number of sources: many are derived from the exploratory voyages of r/v ‘Oceania’, and are available from the Regional Oceanographic Data Bank of IO PAS; some are from the voyages of r/v ‘Profesor Siedlecki’ of the Sea Fisheries Institute, Gdynia, (especially primary production and chlorophyll concentrations) and r/v ‘Akademik Kurchatov’ of the P.P. Shirshov Institute of the Russian Academy of Sciences in Moscow. The data are, among other things, the result of several international experiments (with the participation of these and other research vessels), *e.g.* in the ‘Patchiness Experiment ‘86’ (ICES, 1989), the ‘Experiment Sopot ‘87’ or the ULISSE (Ooms, 1996).

The spectra of reflectance function $R(0^-, \lambda)$ were prepared especially for this calculation by M. Darecki, based on experimental results from the r/v ‘Oceania’ cruises.

3. Results and discussion

Detailed results of the computations of the fourteen mean radiant energy fluxes together with the radiation balance for the sea surface $Q_{15} = Q_9 - Q_{14}$ per 1 m² of surface area Q_i [W m⁻²] for each month of the year are given in Tab. 1. These values were calculated for all twenty sub-regions of the southern Baltic numbered as on the map (Fig. 3). Tab. 1 also gives the annual means of the various energy fluxes.

Table 1. Mean radiant energy fluxes Q_i together with the radiation balance for the sea surface $Q_{15} = Q_9 - Q_{14}$, per 1 m² of surface area [W m⁻²] for each month of the year and for the whole year.

Numbers $i = 1, 2, 3, \dots, 14$ denote the following fluxes (given also in Fig. 1): Q_1 – flux entering the Earth’s atmosphere, Q_2 – flux absorbed in the atmosphere, $Q_{2'}$ – flux scattered upwards (reflected) in the atmosphere, Q_3 – direct solar ray flux reaching the sea surface, Q_4 – diffuse solar flux (scattered downwards in the atmosphere) reaching the sea surface, Q_5 – total solar flux reaching the sea surface, Q_6 – total flux reflected by the sea surface, Q_7 – total flux entering the water column, Q_8 – flux scattered upwards by the water body and leaving the sea surface, Q_9 – flux absorbed in the water column, Q_{10} – flux absorbed by the water itself, Q_{11} – flux absorbed by admixtures other than phytoplankton pigments, Q_{12} – flux absorbed by phytoplankton pigments, Q_{13} – photosynthetically stored radiation flux, Q_{14} – effective infrared radiation flux at the sea surface

Sub-region 1

Flux [W m^{-2}]	Q_1	$Q_{2+2'}$	Q_3	Q_4	Q_5	Q_6	Q_7	Q_8	Q_9	Q_{10}	Q_{11}	Q_{12}	Q_{13}	Q_{14}	Q_{15}
January	70.3	50.2	5.4	14.7	20.1	1.88	18.2	0.053	18.2	12.9	4.6	0.65	0.018	78.5	-60.4
February	136.2	76.1	25.4	34.7	60.1	4.79	55.3	0.161	55.2	38.8	14.3	2.10	0.041	76.6	-21.5
March	230.4	123.6	51.4	55.4	106.8	6.34	100.5	0.306	100.2	67.5	26.9	5.81	0.108	81.8	18.3
April	344.8	142.8	131.1	70.9	201.9	10.06	191.9	0.586	191.3	125.0	48.5	17.75	0.292	81.4	109.8
May	435.3	178.4	173.8	83.1	256.9	11.44	245.5	0.743	244.7	163.2	66.1	15.45	0.270	77.5	167.2
June	480.7	180.7	211.7	88.3	300.0	13.09	286.9	0.833	286.0	193.9	78.7	13.49	0.243	79.5	206.5
July	462.4	177.4	196.6	88.3	285.0	12.14	272.8	0.840	272.0	179.7	74.8	17.47	0.377	78.4	193.5
August	387.6	147.8	168.1	71.6	239.8	11.24	228.5	0.681	227.8	149.3	60.8	17.65	0.427	81.9	145.9
September	281.3	131.7	93.3	56.2	149.6	8.68	140.9	0.437	140.4	92.8	37.4	10.21	0.272	77.9	62.5
October	175.2	106.5	32.8	36.0	68.7	4.90	63.8	0.201	63.6	42.1	16.9	4.53	0.145	78.8	-15.1
November	91.8	65.6	8.2	18.0	26.2	2.43	23.8	0.076	23.7	15.8	6.1	1.81	0.069	81.1	-57.4
December	56.5	41.3	3.7	11.5	15.2	1.71	13.5	0.040	13.5	9.5	3.4	0.57	0.020	82.1	-68.6
annual mean	263.1	118.6	92.0	52.4	144.5	7.39	137.1	0.414	136.6	91.0	36.6	8.99	0.191	79.6	57.1

Sub-region 2

Flux [W m^{-2}]	Q_1	$Q_{2+2'}$	Q_3	Q_4	Q_5	Q_6	Q_7	Q_8	Q_9	Q_{10}	Q_{11}	Q_{12}	Q_{13}	Q_{14}	Q_{15}
January	67.0	46.7	5.5	14.9	20.3	1.93	18.4	0.053	18.4	13.1	4.6	0.67	0.019	85.9	-67.5
February	132.6	85.0	18.0	29.6	47.6	4.00	43.6	0.124	43.5	30.4	11.4	1.71	0.038	71.6	-28.1
March	227.2	118.8	53.2	55.3	108.4	6.56	101.9	0.245	101.6	68.2	27.3	6.09	0.113	78.7	23.0
April	342.5	147.3	124.2	71.0	195.2	9.88	185.3	0.393	184.9	120.1	47.0	17.82	0.298	74.4	110.6
May	434.1	177.8	173.1	83.2	256.3	11.40	244.9	0.584	244.3	162.7	65.7	15.92	0.266	77.4	166.9
June	480.3	176.0	217.6	86.8	304.4	12.91	291.4	0.760	290.6	197.0	79.7	14.00	0.252	81.3	209.4
July	461.8	193.1	178.3	90.3	268.7	11.48	257.2	0.625	256.5	168.5	71.0	17.15	0.376	71.1	185.5
August	385.9	145.8	168.6	71.5	240.1	11.35	228.7	0.518	228.2	149.4	60.5	18.26	0.429	79.8	148.3
September	278.4	121.1	101.5	55.8	157.3	9.19	148.1	0.341	147.7	97.8	38.9	11.02	0.279	83.8	63.9
October	171.8	100.9	34.4	36.4	70.8	5.31	65.5	0.156	65.4	43.3	17.3	4.81	0.154	86.7	-21.4
November	88.4	61.7	8.5	18.3	26.7	2.64	24.1	0.056	24.0	16.0	6.1	1.89	0.073	90.1	-66.1
December	53.3	39.1	3.4	10.9	14.3	1.29	13.0	0.035	12.9	9.1	3.3	0.55	0.021	76.3	-63.4
annual mean	260.7	117.8	90.8	52.1	142.8	7.33	135.5	0.325	135.2	89.8	36.1	9.19	0.194	79.7	55.5

Sub-region 3															
Flux [W m^{-2}]	Q_1	$Q_{2+2'}$	Q_3	Q_4	Q_5	Q_6	Q_7	Q_8	Q_9	Q_{10}	Q_{11}	Q_{12}	Q_{13}	Q_{14}	Q_{15}
January	73.7	48.3	7.5	17.8	25.3	2.41	22.9	0.086	22.8	16.0	5.8	1.01	0.030	84.5	-61.7
February	139.8	81.5	24.0	34.3	58.3	4.33	54.0	0.203	53.8	37.2	14.0	2.57	0.053	83.4	-29.6
March	233.8	132.0	47.2	54.6	101.8	6.12	95.7	0.381	95.3	62.4	25.1	7.77	0.146	72.4	22.9
April	347.0	170.7	106.0	70.4	176.3	9.04	167.3	0.679	166.6	103.8	41.4	21.36	0.399	67.5	99.1
May	436.3	172.3	182.3	81.7	264.0	11.96	252.0	0.987	251.0	163.3	65.4	22.26	0.406	79.4	171.6
June	481.0	186.6	204.4	90.0	294.4	12.38	282.1	1.088	280.9	186.7	76.5	17.67	0.355	81.5	199.4
July	463.1	202.7	170.1	90.3	260.4	11.08	249.3	1.008	248.3	158.7	66.7	22.84	0.582	74.7	173.5
August	389.4	143.4	175.2	70.8	245.9	11.52	234.4	0.941	233.4	148.5	59.5	25.33	0.650	88.2	145.2
September	284.1	133.7	93.8	56.7	150.5	8.61	141.9	0.572	141.3	90.7	36.1	14.51	0.382	81.7	59.6
October	178.6	104.1	36.7	37.8	74.5	5.66	68.8	0.281	68.5	44.3	17.4	6.88	0.214	89.4	-20.9
November	95.3	64.5	10.4	20.3	30.7	2.97	27.8	0.115	27.6	17.8	6.8	2.99	0.109	75.5	-47.9
December	59.7	43.1	4.2	12.3	16.5	1.58	15.0	0.058	14.9	10.3	3.8	0.82	0.031	75.3	-60.4
annual mean	265.5	123.6	88.7	53.1	141.9	7.31	134.5	0.535	134.0	86.8	35.0	12.21	0.281	79.4	54.6

Sub-region 4															
Flux [W m^{-2}]	Q_1	$Q_{2+2'}$	Q_3	Q_4	Q_5	Q_6	Q_7	Q_8	Q_9	Q_{10}	Q_{11}	Q_{12}	Q_{13}	Q_{14}	Q_{15}
January	70.3	50.6	5.3	14.4	19.7	1.76	17.9	0.052	17.9	12.8	4.5	0.60	0.017	87.2	-69.3
February	136.2	80.7	22.4	33.1	55.5	4.19	51.3	0.150	51.2	36.1	13.2	1.87	0.037	79.0	-27.8
March	230.4	129.3	47.0	54.2	101.1	5.92	95.2	0.290	94.9	64.2	25.6	5.12	0.094	82.8	12.1
April	344.8	163.9	110.1	70.8	180.9	9.02	171.8	0.531	171.3	111.9	44.6	14.78	0.251	69.8	101.5
May	435.3	171.1	182.1	82.1	264.2	11.80	252.4	0.756	251.6	169.3	67.8	14.55	0.242	82.3	169.3
June	480.7	183.1	208.5	89.2	297.6	12.56	285.0	0.848	284.1	193.4	78.1	12.63	0.217	84.1	200.0
July	462.4	180.1	194.0	88.3	282.3	12.00	270.3	0.833	269.4	178.6	74.9	15.99	0.359	77.8	191.7
August	387.6	151.6	163.8	72.3	236.0	11.25	224.8	0.694	224.0	147.8	60.4	15.88	0.387	84.3	139.7
September	281.3	120.9	104.7	55.6	160.4	9.21	151.1	0.464	150.6	100.6	40.1	9.91	0.251	89.8	60.9
October	175.2	111.5	29.5	34.2	63.7	4.55	59.1	0.187	58.9	39.2	15.9	3.87	0.126	71.2	-12.3
November	91.8	63.1	9.5	19.3	28.7	2.78	25.9	0.082	25.9	17.4	6.7	1.80	0.066	86.4	-60.6
December	56.5	42.7	3.3	10.5	13.8	1.36	12.4	0.037	12.4	8.8	3.1	0.49	0.017	81.7	-69.3
annual mean	263.1	120.8	90.3	52.0	142.3	7.20	135.1	0.411	134.6	90.2	36.3	8.15	0.173	81.3	53.4

Sub-region 5

Flux [W m^{-2}]	Q_1	$Q_{2+2'}$	Q_3	Q_4	Q_5	Q_6	Q_7	Q_8	Q_9	Q_{10}	Q_{11}	Q_{12}	Q_{13}	Q_{14}	Q_{15}
January	67.0	48.1	5.0	13.9	18.9	1.74	17.2	0.049	17.1	12.2	4.3	0.64	0.020	84.4	-67.3
February	132.6	85.0	18.1	29.6	47.6	3.64	44.0	0.125	43.8	30.6	11.5	1.79	0.040	78.5	-34.7
March	227.2	126.4	47.0	53.8	100.8	5.97	94.8	0.239	94.6	63.2	25.4	6.03	0.114	75.9	18.7
April	342.5	140.2	131.6	70.7	202.2	10.48	191.8	0.407	191.3	124.2	47.8	19.36	0.305	82.8	108.6
May	434.1	179.2	171.1	83.9	255.0	11.35	243.6	0.583	243.0	161.5	64.8	16.77	0.262	76.4	166.6
June	480.3	178.5	214.2	87.6	301.8	12.84	288.9	0.760	288.1	194.4	79.1	14.57	0.267	85.0	203.1
July	461.8	198.8	172.6	90.4	263.0	11.23	251.8	0.619	251.1	163.9	69.3	17.93	0.389	66.8	184.3
August	385.9	151.6	162.0	72.3	234.3	11.02	223.3	0.511	222.8	144.9	58.8	19.05	0.455	78.7	144.1
September	278.4	126.0	96.4	56.0	152.4	8.76	143.6	0.335	143.3	94.2	37.6	11.47	0.302	86.9	56.4
October	171.8	102.7	33.1	36.0	69.0	5.11	63.9	0.153	63.8	42.0	16.7	5.00	0.153	82.2	-18.5
November	88.4	62.1	8.3	18.0	26.3	2.27	24.0	0.056	23.9	15.9	6.1	2.01	0.078	84.4	-60.4
December	53.3	39.4	3.3	10.7	13.9	1.43	12.5	0.034	12.5	8.7	3.2	0.56	0.021	83.3	-70.8
annual mean	260.7	119.9	88.8	52.0	140.7	7.16	133.6	0.323	133.2	88.2	35.5	9.63	0.201	80.3	52.9

Sub-region 6

Flux [W m^{-2}]	Q_1	$Q_{2+2'}$	Q_3	Q_4	Q_5	Q_6	Q_7	Q_8	Q_9	Q_{10}	Q_{11}	Q_{12}	Q_{13}	Q_{14}	Q_{15}
January	70.3	49.7	5.6	15.0	20.7	2.00	18.7	0.056	18.6	12.8	4.8	1.05	0.035	75.3	-56.7
February	136.2	84.9	20.0	31.3	51.3	3.84	47.5	0.139	47.3	33.0	12.5	1.88	0.041	72.2	-24.9
March	230.4	135.3	42.6	52.5	95.1	5.53	89.6	0.268	89.3	60.7	24.4	4.10	0.072	72.4	16.9
April	344.8	150.2	123.2	71.4	194.6	9.69	184.9	0.547	184.3	123.9	49.2	11.28	0.172	73.9	110.4
May	435.3	164.1	191.2	80.0	271.2	12.03	259.2	0.772	258.4	171.4	68.2	18.72	0.304	78.6	179.8
June	480.7	176.0	216.7	87.9	304.7	12.89	291.8	0.869	290.9	193.6	78.2	19.08	0.342	88.0	202.9
July	462.4	189.4	182.9	90.1	273.0	11.58	261.4	0.801	260.6	170.7	71.6	18.26	0.413	76.7	183.9
August	387.6	153.0	162.5	72.2	234.7	10.90	223.8	0.687	223.0	145.2	59.4	18.47	0.453	76.8	146.2
September	281.3	132.8	92.2	56.3	148.5	8.41	140.1	0.430	139.6	91.7	36.8	11.19	0.284	78.7	60.9
October	175.2	99.2	38.1	37.9	76.0	5.84	70.2	0.217	69.9	46.2	18.1	5.70	0.170	89.5	-19.6
November	91.8	66.2	8.0	17.6	25.6	2.36	23.2	0.074	23.2	15.2	5.9	2.10	0.084	74.4	-51.2
December	56.5	41.3	3.7	11.5	15.2	1.49	13.7	0.041	13.6	9.3	3.5	0.88	0.035	83.1	-69.5
annual mean	263.1	120.2	90.8	52.0	142.9	7.22	135.6	0.409	135.2	89.7	36.1	9.43	0.201	78.3	56.9

Sub-region 7															
Flux [W m^{-2}]	Q_1	$Q_{2+2'}$	Q_3	Q_4	Q_5	Q_6	Q_7	Q_8	Q_9	Q_{10}	Q_{11}	Q_{12}	Q_{13}	Q_{14}	Q_{15}
January	67.0	44.7	6.2	16.1	22.3	2.06	20.3	0.052	20.2	14.1	5.1	1.00	0.033	87.0	-66.8
February	132.6	79.0	21.3	32.3	53.6	4.11	49.5	0.144	49.4	34.9	12.7	1.79	0.036	88.5	-39.2
March	227.2	122.5	50.0	54.7	104.7	6.23	98.5	0.279	98.2	67.7	26.4	4.08	0.069	78.8	19.3
April	342.5	136.6	136.1	69.8	205.9	10.47	195.4	0.489	194.9	132.7	51.7	10.48	0.150	80.7	114.1
May	434.1	169.5	182.8	81.8	264.6	11.87	252.8	0.610	252.1	168.6	67.4	16.11	0.255	78.4	173.7
June	480.3	182.6	208.3	89.4	297.7	12.61	285.1	0.712	284.3	190.2	77.6	16.58	0.313	83.9	200.5
July	461.8	180.6	192.4	88.9	281.2	12.05	269.2	0.675	268.5	177.8	74.2	16.46	0.345	74.9	193.5
August	385.9	143.6	171.3	70.9	242.2	11.46	230.8	0.545	230.2	152.0	61.7	16.51	0.399	87.0	143.2
September	278.4	122.4	100.2	55.7	155.9	8.96	147.0	0.350	146.6	97.5	38.9	10.20	0.264	90.2	56.4
October	171.8	103.0	32.9	35.9	68.8	5.14	63.6	0.154	63.5	42.2	16.8	4.53	0.142	86.4	-22.9
November	88.4	63.7	7.6	17.1	24.7	2.15	22.5	0.053	22.5	15.0	5.7	1.75	0.067	83.1	-60.6
December	53.3	38.9	3.4	11.0	14.4	1.56	12.9	0.033	12.8	8.8	3.3	0.73	0.029	83.7	-70.8
annual mean	260.7	115.7	93.0	52.0	145.0	7.40	137.6	0.342	137.2	92.0	36.9	8.38	0.176	83.4	53.8

Sub-region 8															
Flux [W m^{-2}]	Q_1	$Q_{2+2'}$	Q_3	Q_4	Q_5	Q_6	Q_7	Q_8	Q_9	Q_{10}	Q_{11}	Q_{12}	Q_{13}	Q_{14}	Q_{15}
January	73.7	54.7	5.2	13.7	18.9	1.72	17.2	0.066	17.1	11.8	4.4	0.92	0.031	68.8	-51.6
February	139.8	84.3	22.3	33.2	55.5	4.35	51.1	0.190	50.9	35.6	13.3	2.04	0.042	83.9	-33.0
March	233.8	136.8	43.7	53.2	97.0	5.73	91.2	0.350	90.9	61.6	24.8	4.50	0.079	71.6	19.2
April	347.0	147.2	128.3	71.5	199.8	10.02	189.8	0.726	189.0	125.9	49.8	13.31	0.205	75.5	113.6
May	436.3	171.5	182.9	81.9	264.8	11.68	253.1	0.974	252.1	166.8	66.8	18.52	0.321	80.3	171.9
June	481.0	175.9	217.3	87.8	305.1	12.84	292.2	1.114	291.1	194.1	78.4	18.59	0.345	93.2	197.9
July	463.1	200.5	171.6	90.9	262.5	11.16	251.4	0.991	250.3	163.9	68.6	17.87	0.419	82.3	168.1
August	389.4	144.6	173.8	71.0	244.7	11.29	233.4	0.920	232.5	151.5	61.4	19.61	0.481	83.8	148.6
September	284.1	128.8	98.6	56.8	155.4	8.82	146.6	0.580	146.0	95.8	38.2	11.88	0.300	85.5	60.5
October	178.6	106.9	34.6	37.1	71.6	5.12	66.5	0.266	66.2	43.7	17.1	5.45	0.164	93.1	-26.9
November	95.3	68.7	8.4	18.2	26.6	2.60	24.0	0.096	23.9	15.6	6.1	2.19	0.085	71.4	-47.5
December	59.7	42.9	4.3	12.5	16.7	1.53	15.2	0.059	15.2	10.4	3.8	0.94	0.036	78.9	-63.7
annual mean	265.5	122.0	91.1	52.3	143.5	7.24	136.2	0.529	135.7	89.9	36.1	9.68	0.210	80.6	55.1

Sub-region 9

Flux [W m ⁻²]	Q ₁	Q _{2+2'}	Q ₃	Q ₄	Q ₅	Q ₆	Q ₇	Q ₈	Q ₉	Q ₁₀	Q ₁₁	Q ₁₂	Q ₁₃	Q ₁₄	Q ₁₅
January	70.3	52.4	4.8	13.0	17.9	1.74	16.1	0.049	16.1	11.0	4.1	0.97	0.034	67.5	-51.4
February	136.2	81.2	22.1	32.9	55.1	4.30	50.8	0.148	50.6	35.3	13.2	2.08	0.043	78.5	-27.9
March	230.4	130.8	45.9	53.8	99.6	5.89	93.7	0.280	93.4	63.6	25.4	4.47	0.078	76.3	17.2
April	344.8	138.4	136.2	70.2	206.4	10.39	196.0	0.580	195.4	131.3	51.4	12.69	0.187	80.4	115.0
May	435.3	168.1	185.7	81.6	267.2	11.87	255.3	0.766	254.5	168.0	66.6	19.87	0.314	77.7	176.8
June	480.7	165.8	236.1	78.7	314.8	13.34	301.5	0.911	300.5	198.4	80.8	21.38	0.424	82.1	218.4
July	462.4	189.2	183.0	90.2	273.2	11.58	261.6	0.807	260.8	170.0	71.1	19.66	0.454	81.6	179.2
August	387.6	158.6	156.6	72.5	229.1	10.74	218.3	0.678	217.6	140.6	57.5	19.47	0.499	74.9	142.7
September	281.3	126.9	97.9	56.4	154.3	9.21	145.1	0.448	144.7	94.5	37.6	12.49	0.337	89.0	55.7
October	175.2	109.5	30.7	35.0	65.7	4.66	61.0	0.192	60.8	39.8	15.7	5.38	0.174	88.5	-27.7
November	91.8	65.7	8.2	17.9	26.1	2.50	23.6	0.072	23.5	15.3	5.9	2.30	0.091	73.6	-50.1
December	56.5	42.4	3.4	10.7	14.1	1.44	12.6	0.038	12.6	8.6	3.2	0.87	0.036	83.2	-70.6
annual mean	263.1	119.2	92.7	51.1	143.8	7.30	136.5	0.415	136.1	89.8	36.1	10.17	0.223	79.3	56.8

Sub-region 10

Flux [W m ⁻²]	Q ₁	Q _{2+2'}	Q ₃	Q ₄	Q ₅	Q ₆	Q ₇	Q ₈	Q ₉	Q ₁₀	Q ₁₁	Q ₁₂	Q ₁₃	Q ₁₄	Q ₁₅
January	67.0	49.7	4.6	12.8	17.3	1.60	15.7	0.042	15.7	10.8	4.0	0.84	0.030	73.0	-57.3
February	132.6	81.3	20.0	31.3	51.3	4.14	47.2	0.141	47.0	33.1	12.2	1.78	0.038	85.8	-38.8
March	227.2	129.7	44.6	53.0	97.5	5.82	91.7	0.267	91.4	62.6	24.8	4.00	0.068	74.1	17.3
April	342.5	158.4	112.8	71.2	184.1	9.67	174.4	0.450	173.9	117.4	46.5	10.05	0.152	75.9	98.1
May	434.1	190.3	159.3	84.6	243.8	10.92	232.9	0.580	232.3	154.0	62.2	16.02	0.253	71.4	160.8
June	480.3	173.6	221.5	85.3	306.8	13.06	293.7	0.750	292.9	195.1	79.5	18.22	0.345	82.2	210.8
July	461.8	179.5	193.3	89.1	282.3	12.05	270.3	0.690	269.6	178.1	73.9	17.63	0.374	82.3	187.3
August	385.9	147.0	167.2	71.7	238.9	11.24	227.6	0.552	227.0	149.0	60.5	17.57	0.420	84.1	143.0
September	278.4	121.9	100.9	55.6	156.4	9.09	147.3	0.360	147.0	97.2	38.8	11.01	0.283	87.4	59.5
October	171.8	100.6	34.6	36.6	71.2	5.24	66.0	0.162	65.8	43.7	17.1	5.02	0.157	88.2	-22.4
November	88.4	62.7	8.0	17.7	25.6	2.19	23.5	0.057	23.4	15.5	5.9	1.96	0.076	81.9	-58.5
December	53.3	40.5	3.0	9.9	12.9	1.24	11.6	0.030	11.6	8.0	2.9	0.70	0.029	81.2	-69.6
annual mean	260.7	119.7	89.4	51.6	141.0	7.19	133.8	0.341	133.4	88.9	35.8	8.77	0.186	80.5	52.9

Sub-region 11

Flux [W m^{-2}]	Q_1	$Q_{2+2'}$	Q_3	Q_4	Q_5	Q_6	Q_7	Q_8	Q_9	Q_{10}	Q_{11}	Q_{12}	Q_{13}	Q_{14}	Q_{15}
January	70.3	52.7	4.8	12.9	17.6	1.67	16.0	0.047	15.9	11.2	4.1	0.69	0.022	75.0	-59.1
February	136.2	81.7	21.9	32.7	54.6	4.49	50.1	0.146	49.9	35.2	13.0	1.78	0.034	74.6	-24.6
March	230.4	116.4	57.6	56.4	114.0	6.86	107.2	0.314	106.9	74.2	28.5	4.18	0.063	86.5	20.4
April	344.8	155.2	117.9	71.6	189.6	9.50	180.0	0.538	179.5	120.8	47.9	10.79	0.169	79.2	100.3
May	435.3	182.1	169.4	83.9	253.2	11.19	242.0	0.733	241.2	160.0	64.6	16.59	0.275	75.4	165.8
June	480.7	198.4	189.8	92.4	282.3	11.97	270.3	0.819	269.4	179.5	73.8	16.12	0.290	79.7	189.7
July	462.4	185.3	187.6	89.5	277.1	11.79	265.3	0.817	264.5	175.0	73.4	16.09	0.365	77.8	186.6
August	387.6	154.4	161.0	72.3	233.3	10.90	222.4	0.683	221.6	146.7	60.3	14.59	0.360	81.6	140.0
September	281.3	124.1	100.8	56.5	157.2	9.28	147.9	0.450	147.4	98.8	39.2	9.48	0.236	95.1	52.3
October	175.2	114.1	28.0	33.2	61.2	4.47	56.7	0.178	56.5	37.6	15.0	3.90	0.127	82.2	-25.7
November	91.8	65.8	8.1	17.8	26.0	2.34	23.6	0.074	23.5	15.9	6.1	1.55	0.057	79.5	-55.9
December	56.5	42.9	3.3	10.3	13.6	1.27	12.3	0.037	12.3	8.6	3.1	0.58	0.022	73.8	-61.5
annual mean	263.1	122.8	87.8	52.5	140.3	7.15	133.1	0.404	132.7	88.8	35.8	8.06	0.169	79.9	52.7

Sub-region 12

Flux [W m^{-2}]	Q_1	$Q_{2+2'}$	Q_3	Q_4	Q_5	Q_6	Q_7	Q_8	Q_9	Q_{10}	Q_{11}	Q_{12}	Q_{13}	Q_{14}	Q_{15}
January	67.0	50.7	4.3	11.9	16.3	1.48	14.8	0.038	14.8	10.2	3.8	0.80	0.029	67.9	-53.2
February	132.6	82.7	19.3	30.7	50.0	3.79	46.2	0.131	46.0	32.1	12.0	1.89	0.042	79.8	-33.7
March	227.2	109.7	61.0	56.5	117.5	7.15	110.4	0.299	110.1	75.7	29.3	5.03	0.083	88.8	21.2
April	342.5	158.9	112.6	71.1	183.6	9.17	174.4	0.413	174.0	115.2	45.8	13.08	0.214	76.6	97.4
May	434.1	176.4	174.2	83.5	257.7	11.51	246.2	0.557	245.6	160.6	63.8	21.23	0.349	78.3	167.3
June	480.3	175.2	218.8	86.2	305.1	12.91	292.2	0.688	291.4	191.6	77.8	21.94	0.430	84.1	207.3
July	461.8	174.2	199.7	87.8	287.6	12.28	275.3	0.652	274.6	179.3	74.0	21.20	0.463	83.6	190.9
August	385.9	152.3	161.4	72.2	233.6	10.96	222.6	0.509	222.1	144.2	58.8	19.12	0.475	78.8	143.2
September	278.4	136.3	86.7	55.4	142.1	8.11	134.0	0.308	133.6	87.4	34.9	11.35	0.291	79.8	53.9
October	171.8	95.4	38.8	37.5	76.3	5.67	70.7	0.161	70.5	46.2	18.0	6.24	0.192	90.6	-20.2
November	88.4	64.2	7.4	16.9	24.2	2.06	22.2	0.051	22.1	14.6	5.6	1.94	0.076	79.6	-57.5
December	53.3	40.6	3.0	9.8	12.8	1.20	11.6	0.029	11.5	7.9	2.9	0.71	0.030	74.8	-63.2
annual mean	260.7	118.1	90.9	51.7	142.6	7.20	135.4	0.320	135.1	89.0	35.7	10.42	0.224	80.2	54.9

Sub-region 13

Flux [W m^{-2}]	Q_1	$Q_{2+2'}$	Q_3	Q_4	Q_5	Q_6	Q_7	Q_8	Q_9	Q_{10}	Q_{11}	Q_{12}	Q_{13}	Q_{14}	Q_{15}
January	72.8	51.0	6.1	15.8	21.9	2.12	19.8	0.074	19.7	13.8	5.0	0.82	0.024	78.4	-58.7
February	138.9	87.6	20.0	31.3	51.3	4.13	47.2	0.181	47.0	32.2	12.3	2.47	0.058	78.1	-31.1
March	233.0	110.2	65.7	57.1	122.7	7.71	115.0	0.459	114.5	74.2	28.7	11.63	0.214	77.9	36.7
April	346.5	156.2	118.6	71.8	190.3	9.43	180.9	0.749	180.1	105.5	43.4	31.20	0.574	78.2	101.9
May	436.1	177.1	175.5	83.5	259.0	11.51	247.5	0.996	246.5	153.6	60.6	32.27	0.621	85.5	160.9
June	480.9	196.5	192.8	91.6	284.4	12.07	272.4	1.096	271.2	172.3	70.0	28.92	0.662	83.2	188.0
July	462.8	185.3	187.5	90.0	277.6	11.95	265.6	1.087	264.5	164.4	67.3	32.78	0.781	82.8	181.7
August	388.9	157.1	159.0	72.7	231.8	10.85	220.9	0.878	220.0	143.3	58.3	18.28	0.466	86.4	133.6
September	283.4	132.5	94.4	56.5	150.9	8.68	142.2	0.570	141.6	92.2	36.7	12.77	0.347	86.7	55.0
October	177.8	101.8	38.0	38.0	76.0	5.75	70.2	0.281	69.9	46.3	18.1	5.55	0.170	95.3	-25.3
November	94.4	66.0	9.3	19.2	28.5	2.75	25.7	0.103	25.6	17.3	6.6	1.69	0.060	89.5	-63.9
December	58.9	43.0	4.0	11.9	15.9	1.63	14.3	0.055	14.2	10.0	3.6	0.64	0.023	85.9	-71.7
annual mean	264.9	122.0	89.6	53.3	142.9	7.39	135.5	0.546	134.9	85.7	34.3	14.97	0.335	83.9	51.0

Sub-region 14

Flux [W m^{-2}]	Q_1	$Q_{2+2'}$	Q_3	Q_4	Q_5	Q_6	Q_7	Q_8	Q_9	Q_{10}	Q_{11}	Q_{12}	Q_{13}	Q_{14}	Q_{15}
January	70.3	48.6	6.0	15.7	21.7	2.16	19.5	0.058	19.5	13.4	5.0	1.10	0.036	80.0	-60.5
February	136.2	80.8	22.3	33.0	55.4	4.45	50.9	0.149	50.8	34.9	13.3	2.60	0.059	79.8	-29.1
March	230.4	111.8	61.8	56.8	118.6	7.34	111.3	0.327	110.9	75.3	29.5	6.15	0.104	82.3	28.6
April	344.8	147.2	126.0	71.5	197.6	12.01	185.5	0.562	185.0	117.4	45.3	22.24	0.373	81.8	103.1
May	435.3	175.2	177.3	82.8	260.1	11.98	248.2	0.763	247.4	153.9	61.0	32.45	0.575	78.0	169.4
June	480.7	182.1	209.9	88.7	298.6	15.98	282.6	0.866	281.7	178.2	71.6	31.87	0.641	80.3	201.4
July	462.4	184.7	188.1	89.6	277.7	11.84	265.9	0.827	265.0	166.8	68.6	29.58	0.720	82.4	182.6
August	387.6	152.3	163.2	72.1	235.3	13.57	221.7	0.686	221.0	140.0	56.6	24.41	0.635	80.2	140.8
September	281.3	125.5	99.7	56.1	155.7	9.18	146.6	0.453	146.1	93.0	36.8	16.36	0.450	84.9	61.2
October	175.2	101.3	36.5	37.3	73.9	5.53	68.4	0.215	68.1	43.1	16.8	8.31	0.266	87.4	-19.3
November	91.8	62.8	9.6	19.4	29.0	2.69	26.3	0.082	26.2	17.2	6.5	2.57	0.097	93.1	-66.8
December	56.5	41.1	3.8	11.6	15.4	1.52	13.9	0.041	13.8	9.5	3.5	0.89	0.035	83.1	-69.3
annual mean	263.1	117.8	92.3	52.9	145.2	8.19	137.0	0.420	136.6	87.1	34.6	14.92	0.334	82.7	53.9

Sub-region 15

Flux [W m^{-2}]	Q_1	$Q_{2+2'}$	Q_3	Q_4	Q_5	Q_6	Q_7	Q_8	Q_9	Q_{10}	Q_{11}	Q_{12}	Q_{13}	Q_{14}	Q_{15}
January	67.0	49.6	4.6	12.8	17.4	1.54	15.9	0.047	15.8	11.0	4.1	0.73	0.025	70.4	-54.6
February	132.6	80.4	20.5	31.7	52.3	4.18	48.1	0.142	47.9	33.3	12.6	2.06	0.045	76.2	-28.3
March	227.2	124.8	48.2	54.3	102.4	6.13	96.3	0.287	96.0	65.5	26.0	4.48	0.075	72.6	23.4
April	342.5	134.1	138.5	69.9	208.4	10.54	197.8	0.571	197.2	129.1	49.3	18.82	0.291	86.1	111.2
May	434.1	171.6	179.5	82.9	262.5	11.77	250.7	0.764	249.9	160.6	62.8	26.48	0.428	79.8	170.1
June	480.3	203.0	184.9	92.4	277.3	11.78	265.5	0.820	264.6	170.7	70.0	23.88	0.497	78.9	185.7
July	461.8	210.2	161.5	90.1	251.6	10.73	240.8	0.755	240.0	153.9	64.8	21.33	0.501	66.6	173.5
August	385.9	159.6	153.8	72.5	226.3	11.21	215.1	0.665	214.4	139.0	56.8	18.64	0.465	73.3	141.1
September	278.4	145.7	79.3	53.3	132.6	7.66	125.0	0.391	124.6	80.8	32.7	11.11	0.316	70.7	53.9
October	171.8	112.8	26.7	32.2	58.9	4.21	54.7	0.167	54.5	35.3	13.9	5.34	0.183	79.7	-25.2
November	88.4	65.3	7.0	16.1	23.1	1.94	21.2	0.066	21.1	14.1	5.4	1.61	0.062	82.3	-61.2
December	53.3	41.9	2.8	8.7	11.5	1.25	10.2	0.030	10.2	7.1	2.6	0.51	0.021	72.0	-61.8
annual mean	260.7	125.0	84.2	51.4	135.6	6.92	128.7	0.393	128.3	83.5	33.5	11.28	0.243	75.6	52.7

Sub-region 16

Flux [W m^{-2}]	Q_1	$Q_{2+2'}$	Q_3	Q_4	Q_5	Q_6	Q_7	Q_8	Q_9	Q_{10}	Q_{11}	Q_{12}	Q_{13}	Q_{14}	Q_{15}
January	63.8	46.1	4.5	13.1	17.7	1.60	16.1	0.044	16.0	11.3	4.1	0.65	0.020	72.3	-56.3
February	129.1	73.5	22.7	32.8	55.6	4.37	51.2	0.146	51.0	35.8	13.2	1.97	0.041	84.9	-33.9
March	224.0	113.7	55.1	55.2	110.3	6.99	103.3	0.290	103.0	71.2	27.5	4.27	0.069	81.3	21.7
April	340.0	134.8	135.9	69.3	205.3	10.50	194.8	0.433	194.3	128.8	49.8	15.80	0.243	81.9	112.5
May	433.0	159.8	194.7	78.5	273.2	12.64	260.5	0.565	259.9	169.9	66.6	23.43	0.395	83.7	176.2
June	480.1	180.9	210.5	88.7	299.2	12.75	286.4	0.665	285.7	187.8	76.3	21.58	0.449	89.1	196.6
July	461.2	201.6	168.9	90.7	259.6	11.17	248.5	0.593	247.8	161.6	67.8	18.48	0.421	76.5	171.4
August	384.1	158.5	153.3	72.4	225.7	10.69	215.0	0.509	214.4	140.9	57.9	15.70	0.384	75.3	139.2
September	275.5	140.5	81.1	53.9	134.9	7.77	127.2	0.301	126.9	83.4	33.9	9.51	0.261	74.5	52.3
October	168.3	94.1	37.4	36.8	74.2	5.58	68.6	0.158	68.4	45.2	17.7	5.60	0.173	89.4	-21.0
November	85.0	63.5	6.3	15.2	21.5	1.87	19.6	0.049	19.6	13.2	5.1	1.27	0.048	72.3	-52.7
December	50.2	39.1	2.6	8.5	11.1	1.12	10.0	0.027	9.9	7.0	2.5	0.44	0.017	89.9	-80.0
annual mean	258.2	117.3	89.7	51.3	141.0	7.26	133.7	0.316	133.4	88.2	35.3	9.92	0.211	80.8	52.5

Sub-region 17

Flux [W m^{-2}]	Q_1	$Q_{2+2'}$	Q_3	Q_4	Q_5	Q_6	Q_7	Q_8	Q_9	Q_{10}	Q_{11}	Q_{12}	Q_{13}	Q_{14}	Q_{15}
January	72.8	53.4	5.3	14.1	19.4	1.93	17.5	0.066	17.4	12.2	4.5	0.79	0.025	73.8	-56.4
February	138.9	85.6	21.1	32.2	53.3	4.28	49.0	0.190	48.8	33.1	12.8	2.86	0.068	78.1	-29.3
March	233.0	116.9	59.0	57.1	116.1	7.05	109.0	0.439	108.5	69.3	26.9	12.31	0.234	81.2	27.3
April	346.5	149.7	125.3	71.5	196.8	9.76	187.0	0.779	186.2	107.2	45.0	34.04	0.631	77.4	108.8
May	436.1	165.3	191.0	79.8	270.8	12.27	258.5	1.046	257.4	157.9	62.9	36.67	0.719	79.5	177.9
June	480.9	205.6	183.2	92.1	275.3	11.64	263.7	1.073	262.5	164.0	67.3	31.24	0.693	71.2	191.3
July	462.8	179.9	194.1	88.8	282.9	12.00	270.9	1.116	269.7	165.0	68.0	36.66	0.900	82.4	187.3
August	388.9	147.8	168.9	72.1	241.1	11.24	229.9	0.913	228.9	148.1	59.5	21.31	0.555	91.4	137.5
September	283.4	135.2	91.7	56.5	148.2	8.52	139.7	0.562	139.1	89.6	35.5	14.06	0.388	87.7	51.5
October	177.8	96.3	42.5	38.9	81.5	6.37	75.1	0.300	74.8	49.2	18.9	6.65	0.204	102.6	-27.8
November	94.4	69.6	7.7	17.1	24.8	2.26	22.6	0.091	22.5	15.0	5.8	1.68	0.064	89.1	-66.6
December	58.9	42.3	4.2	12.4	16.6	1.59	15.0	0.057	14.9	10.4	3.7	0.73	0.027	92.8	-77.9
annual mean	264.9	120.6	91.5	52.8	144.3	7.42	136.9	0.554	136.3	85.3	34.3	16.64	0.377	83.9	52.4

Sub-region 18

Flux [W m^{-2}]	Q_1	$Q_{2+2'}$	Q_3	Q_4	Q_5	Q_6	Q_7	Q_8	Q_9	Q_{10}	Q_{11}	Q_{12}	Q_{13}	Q_{14}	Q_{15}
January	70.3	52.4	4.8	13.0	17.9	1.74	16.2	0.059	16.1	11.6	4.0	0.50	0.014	76.9	-60.8
February	136.2	77.5	24.5	34.3	58.7	4.51	54.2	0.196	54.0	38.4	13.8	1.77	0.032	85.5	-31.5
March	230.4	117.8	56.4	56.2	112.7	6.80	105.9	0.407	105.4	71.5	28.4	5.60	0.098	76.7	28.7
April	344.8	154.4	118.9	71.5	190.4	9.58	180.8	0.739	180.0	110.2	43.7	26.15	0.452	75.1	104.9
May	435.3	164.4	190.9	80.0	270.9	12.15	258.8	1.042	257.7	160.9	63.1	33.68	0.604	83.9	173.7
June	480.7	213.0	175.2	92.4	267.6	11.36	256.3	1.031	255.2	164.2	67.9	23.16	0.505	74.0	181.2
July	462.4	188.1	184.4	89.9	274.2	11.77	262.5	1.060	261.3	167.8	69.8	23.80	0.561	77.7	183.6
August	387.6	154.2	160.8	72.6	233.4	10.96	222.4	0.883	221.5	145.1	59.1	17.24	0.432	83.7	137.8
September	281.3	135.0	90.2	56.0	146.2	8.52	137.7	0.548	137.1	90.7	36.5	10.02	0.268	84.3	52.8
October	175.2	100.4	37.3	37.6	74.9	5.59	69.3	0.277	69.0	46.1	18.2	4.66	0.142	91.7	-22.7
November	91.8	66.6	7.8	17.4	25.2	2.33	22.8	0.093	22.7	15.2	5.9	1.64	0.064	86.5	-63.8
December	56.5	42.7	3.3	10.5	13.8	1.29	12.5	0.046	12.5	8.9	3.1	0.42	0.014	79.4	-66.9
annual mean	263.1	122.2	88.2	52.6	140.8	7.22	133.6	0.533	133.0	86.1	34.5	12.43	0.266	81.2	51.9

Sub-region 19

Flux [W m^{-2}]	Q_1	$Q_{2+2'}$	Q_3	Q_4	Q_5	Q_6	Q_7	Q_8	Q_9	Q_{10}	Q_{11}	Q_{12}	Q_{13}	Q_{14}	Q_{15}
January	67.0	50.0	4.5	12.5	17.0	1.68	15.4	0.045	15.3	10.9	3.9	0.57	0.018	80.9	-65.6
February	132.6	74.8	24.0	33.8	57.8	4.56	53.2	0.154	53.1	37.6	13.7	1.88	0.037	88.4	-35.3
March	227.2	122.3	50.2	54.7	104.9	6.21	98.7	0.292	98.4	68.2	26.4	3.77	0.059	77.8	20.6
April	342.5	136.7	136.0	69.7	205.8	10.43	195.4	0.587	194.7	130.3	50.8	13.62	0.199	80.0	114.8
May	434.1	169.1	183.2	81.9	265.0	11.87	253.2	0.770	252.3	166.6	66.2	19.58	0.316	81.5	170.8
June	480.3	187.4	202.7	90.2	292.9	12.54	280.4	0.858	279.5	185.3	76.0	18.18	0.364	85.6	193.9
July	461.8	182.4	190.4	89.0	279.4	11.93	267.5	0.829	266.6	175.9	73.7	16.98	0.381	78.2	188.4
August	385.9	143.0	171.9	71.0	242.9	11.46	231.4	0.707	230.7	153.9	62.5	14.32	0.339	88.3	142.4
September	278.4	133.7	89.0	55.7	144.7	8.27	136.4	0.421	136.0	90.8	36.6	8.64	0.225	84.0	52.0
October	171.8	95.3	38.9	37.6	76.5	5.64	70.9	0.220	70.6	47.3	18.5	4.89	0.147	91.5	-20.9
November	88.4	65.3	6.9	16.1	23.1	2.08	21.0	0.066	20.9	14.3	5.5	1.16	0.044	82.3	-61.4
December	53.3	39.1	3.4	10.9	14.3	1.34	12.9	0.038	12.9	9.1	3.2	0.51	0.018	93.8	-80.9
annual mean	260.7	116.7	92.0	52.0	144.0	7.34	136.7	0.417	136.2	91.0	36.5	8.70	0.180	84.3	52.0

Sub-region 20

Flux [W m^{-2}]	Q_1	$Q_{2+2'}$	Q_3	Q_4	Q_5	Q_6	Q_7	Q_8	Q_9	Q_{10}	Q_{11}	Q_{12}	Q_{13}	Q_{14}	Q_{15}
January	63.8	47.2	4.3	12.3	16.6	1.51	15.1	0.042	15.0	10.7	3.8	0.56	0.017	79.1	-64.0
February	129.1	72.0	23.7	33.3	57.1	4.68	52.4	0.150	52.2	37.0	13.4	1.85	0.036	87.7	-35.5
March	224.0	97.8	70.7	55.5	126.2	7.99	118.2	0.328	117.9	82.7	30.8	4.42	0.067	86.1	31.8
April	340.0	136.2	134.4	69.5	203.9	10.43	193.4	0.435	193.0	129.0	50.3	13.65	0.199	80.8	112.2
May	433.0	171.6	179.0	82.4	261.4	12.00	249.4	0.550	248.8	164.1	65.3	19.52	0.319	81.5	167.3
June	480.1	190.7	198.4	91.0	289.4	12.39	277.0	0.653	276.3	182.9	75.2	18.19	0.368	84.2	192.1
July	461.2	181.5	190.4	89.3	279.7	12.37	267.4	0.639	266.7	176.2	73.4	17.10	0.375	82.3	184.4
August	384.1	142.4	170.8	71.0	241.7	11.52	230.2	0.544	229.6	153.2	62.0	14.39	0.340	91.6	138.0
September	275.5	127.8	91.9	55.8	147.6	8.56	139.1	0.328	138.7	92.7	37.1	8.89	0.227	87.1	51.6
October	168.3	97.0	34.9	36.3	71.3	5.27	66.0	0.154	65.8	43.9	17.3	4.64	0.141	85.3	-19.4
November	85.0	63.7	6.2	15.0	21.3	1.92	19.4	0.048	19.3	13.2	5.0	1.08	0.041	79.8	-60.5
December	50.2	37.4	2.9	9.9	12.8	1.17	11.7	0.031	11.6	8.3	2.9	0.46	0.017	88.2	-76.6
annual mean	258.2	113.8	92.6	51.8	144.4	7.49	136.9	0.326	136.6	91.3	36.5	8.76	0.180	84.4	52.2

The spatial differences and temporal variabilities of the various fluxes and the overall radiant energy balance can be illustrated on the basis of these results. Graphs exemplifying some of the results will be presented below, with the mean fluxes given in $[W m^{-2}]$ or given as mean daily (or yearly) energy doses per $1 m^2$ of surface area $[J m^{-2} day^{-1}]$.

Fig. 4 illustrates how the proportions of some of the mean diurnal energy fluxes vary during the year in the Gdańsk Deep (sub-region 18 in Fig. 3). It shows the energies of the following fluxes – $Q_2 + Q_{2'}$ – the energy absorbed and reflected in the atmosphere, Q_6 – the energy reflected by the surface of the sea, Q_9 – the overall energy absorbed by seawater and its components: Q_{10} – the energy absorbed by the water itself, Q_{12} – the energy absorbed by the phytoplankton, Q_{11} – the energy absorbed by the remaining constituents of the water, and Q_{13} – the energy consumed in primary production – relative to the solar energy reaching the Earth’s atmosphere.

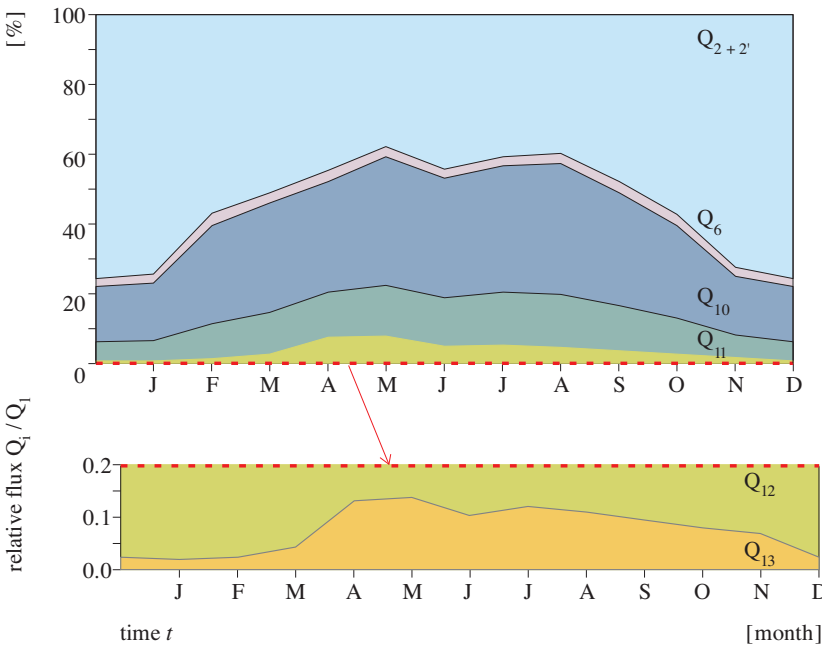


Fig. 4. Seasonal variation of the fluxes related to the solar flux $(Q_i/Q_1) = f(t)$, the percentage of particular flux in relation to the flux reaching the atmosphere is represented by appropriate coloured area; example for sub-region 18 (Gdańsk Deep)

Obviously, in the summer months, a far smaller percentage of the incoming solar energy is absorbed and reflected in the atmosphere, and a larger one reaches the sea surface. There are two reasons for this. Firstly,

the mean cloudiness over the Baltic in winter is much greater than in summer and, moreover, the proportion of low clouds in the overall cloud cover is larger then. Secondly, the winter sun's rays are incident on the Earth at smaller angles. Although these features are generally recognised and can be predicted from the known patterns of weather changes, our calculations show the averaged variations in the proportions of these energy fluxes in the southern Baltic in a quantitative fashion.

The magnitudes of the energy reflected from the sea surface do not alter much during the year. On average they make up around 2% of the energy at the Earth's atmosphere boundary, although instantaneous values of Q_6/Q_1 can range from 1% to 10%.

The total diurnal energies absorbed by the water depend on meteorological factors, *i.e.* they are regulated by the transmission of solar radiation through the atmosphere. Nevertheless, the proportions of energy absorbed by the separate components of seawater depend on the annual cycle of biomass concentration changes in the sea. It is clear from Fig. 4 that both the proportion of energy absorbed by phytoplankton pigments and that stored during the photosynthesis of organic matter rise considerably during the spring blooms and remain at a high level until the autumn.

Tab. 2 sets out the numerical values of these proportions in the various months for a selected sub-region (No. 18 – the Gdańsk Deep).

Table 2. The mean values of particular energy fluxes Q_i as a percentage of the energy reaching the Earth's atmosphere Q_1 (*e.g.* Q_i/Q_1 in %). Example for sub-region 18

Month	2+2'	3	4	5	6	7	8	9	10	11	12	13
January	74.6	6.9	18.5	25.4	2.48	23.0	0.084	22.9	16.4	5.7	0.72	0.019
February	56.9	17.9	25.2	43.1	3.31	39.8	0.144	39.6	28.2	10.1	1.30	0.024
March	51.1	24.5	24.4	48.9	2.95	45.9	0.176	45.8	31.0	12.3	2.43	0.043
April	44.8	34.5	20.7	55.2	2.78	52.4	0.214	52.2	32.0	12.7	7.58	0.131
May	37.8	43.9	18.4	62.2	2.79	59.4	0.239	59.2	37.0	14.5	7.74	0.139
June	44.3	36.5	19.2	55.7	2.36	53.3	0.215	53.1	34.2	14.1	4.81	0.105
July	40.7	39.9	19.4	59.3	2.54	56.8	0.229	56.5	36.3	15.1	5.15	0.121
August	39.8	41.5	18.7	60.2	2.83	57.4	0.228	57.1	37.4	15.3	4.45	0.111
September	48.0	32.1	19.9	52.0	3.03	49.0	0.195	48.8	32.2	13.0	3.56	0.095
October	57.3	21.3	21.4	42.7	3.19	39.5	0.158	39.4	26.3	10.4	2.66	0.081
November	72.6	8.5	18.9	27.4	2.54	24.9	0.101	24.8	16.6	6.4	1.78	0.069
December	75.6	5.9	18.5	24.4	2.27	22.1	0.082	22.1	15.8	5.5	0.74	0.024
year	46.5	33.5	20.0	53.5	2.75	50.8	0.203	50.6	32.7	13.1	4.72	0.101

Variations in the chlorophyll *a* concentration (and hence in the biomass) in the water affect the absorption of radiant energy in the surface seawater. With the aid of this model it has been calculated, and is shown in Fig. 5, how for selected concentrations of chlorophyll *a* (approximating to the average and extreme values measured in the Baltic) the energy absorption distribution varies with depth in the sea. For example, at high concentrations of chlorophyll, 80% of the radiant energy penetrating the sea surface is absorbed in the first 0.7 m of water. When concentrations are low, this depth increases to around 3 m.

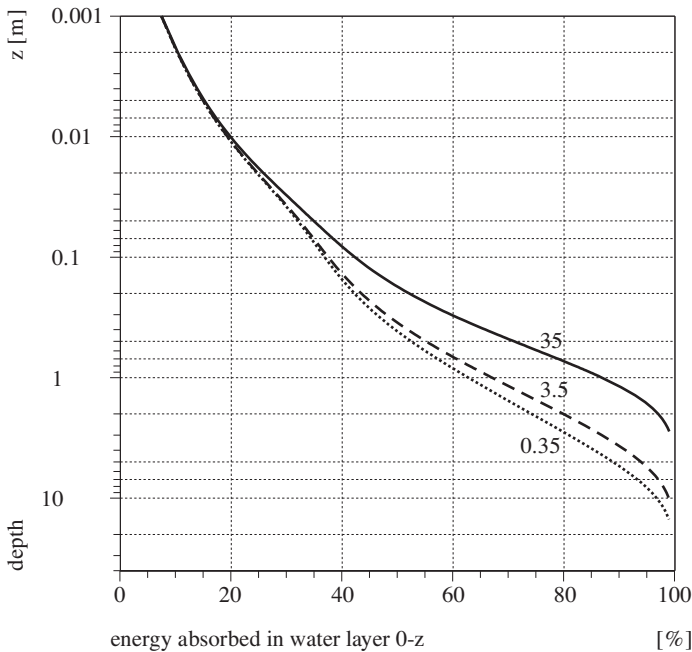


Fig. 5. Radiation absorbed in the water column, example for 3 different surface chlorophyll concentrations $C_a(0)$: 35 mg m^{-3} , 3.5 mg m^{-3} and 0.35 mg m^{-3}

Fig. 6 shows the spatial distributions of the total solar energy flux absorbed by the sea Q_9 for the winter and summer solstice months (December – Fig. 6a, June – Fig. 6b). The colossal differences in the amounts of energy absorbed by the sea between winter and summer are obvious, as is a certain spatial differentiation, though this is small in comparison to the absolute energy values. In view of the low spatial density of data (the mid-points of each sub-region are considered – a total of 20 points), the layout of the isolines on the maps should be treated as giving a rough idea of the situation. Nevertheless, certain regularities can be inferred from them.

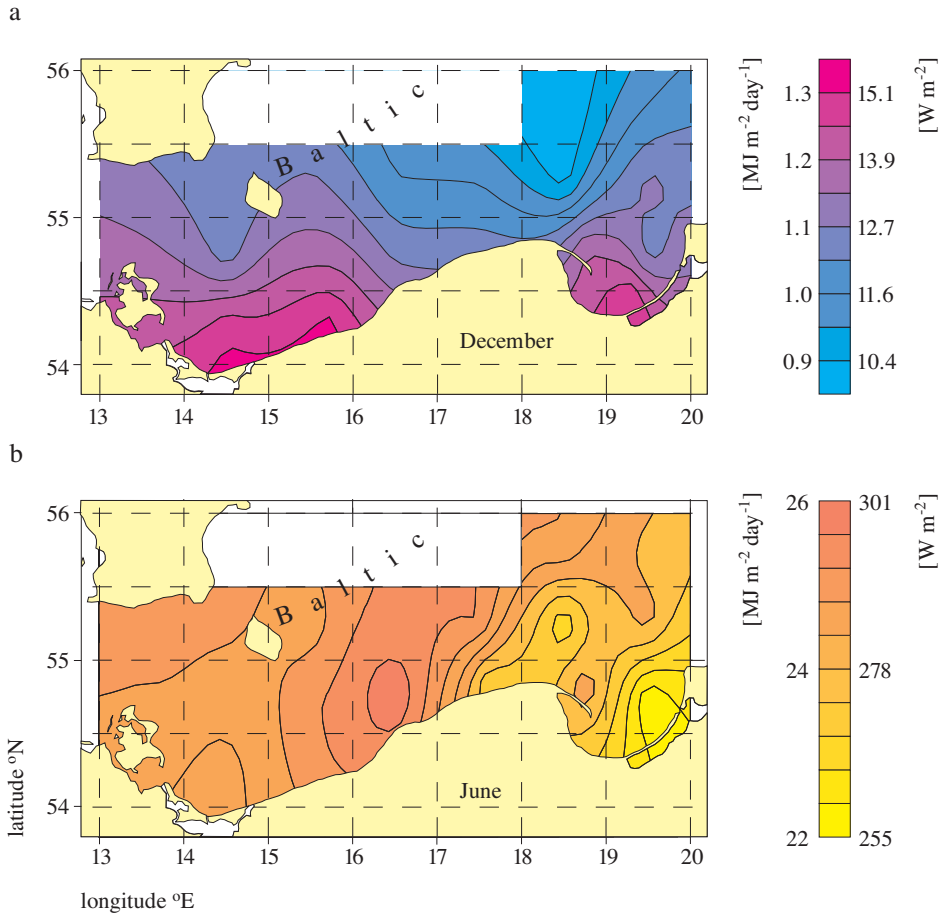


Fig. 6. Solar radiation absorbed in the southern Baltic Q_9 – average distribution in December (a), June (b)

In December there is an evident latitudinal distribution of the variations in absorbed energy, which tends to fall off in the northward direction and which accords with the ever lower position of the Sun above the horizon. In summer (in June), the isolines of energy absorbed by the sea tend to fall off from the open sea towards the shores. But this is a complex situation and, as has been mentioned before, may be encumbered with errors inherent in the graph. The reason for such a distribution is probably the spatial differentiation in the cloud cover. It is known that in summer the mean transmittance of the atmosphere with respect to solar irradiance over the Baltic is greater than that over the land, which can be accounted for by the mechanism of cloud formation (Dera and Rozwadowska, 1991).

The photosynthetically stored radiation (PSR) Q_{13} shown in Fig. 7 is dependent only to a limited extent on the above-mentioned climatic factors. The diagram shows clearly that the annual PSR is highest around the mouths of large rivers. In all probability, the factor principally responsible for controlling the accumulation of energy during photosynthesis is the inflow of nutrients from these rivers. In the entire study region, the amount of energy used up in photosynthesis during the year is scarcely 0.37% of the energy absorbed by the water during this time.

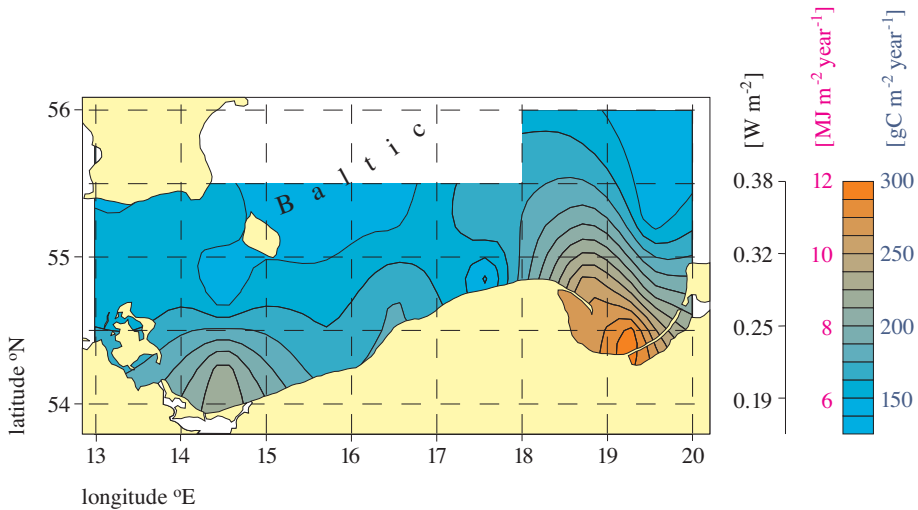


Fig. 7. Photosynthetically stored radiation (PSR) Q_{13} – spatial distribution of annual totals

A significant quantity from the climatological point of view is the radiation balance for the sea surface, *i.e.* the difference between the energy absorbed below the sea surface and the energy effectively radiated by this surface $Q_{15} = Q_9 - Q_{14}$. According to our calculations, the mean annual value of this balance in the southern Baltic is clearly positive – *ca* 1.7 GJ m⁻² year⁻¹ (or in average 53.9 W m⁻²). This makes up some 20% of the total solar energy re-emitted into the atmosphere from this part of the Baltic. The spatial variations in the annual value of this balance in the study area (Fig. 8) are but slight, since its latitudinal extent is rather small. This differentiation resembles the picture in Fig. 6b, *i.e.* the spatial differentiation in the energy absorbed by the sea in June. Obviously, the summer values of absorbed energy, which are a whole order of magnitude larger than the winter values, must affect the annual energy balance at the sea surface to a greater degree. However, the balance $Q_{15} = Q_9 - Q_{14}$ for particular

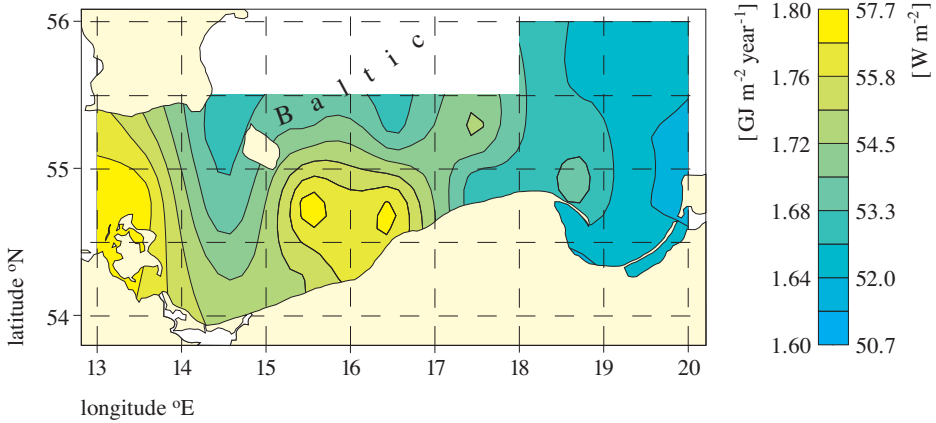


Fig. 8. Radiative energy balance $Q_{15} = Q_9 - Q_{14}$ at the surface of the southern Baltic – spatial distribution of mean annual totals

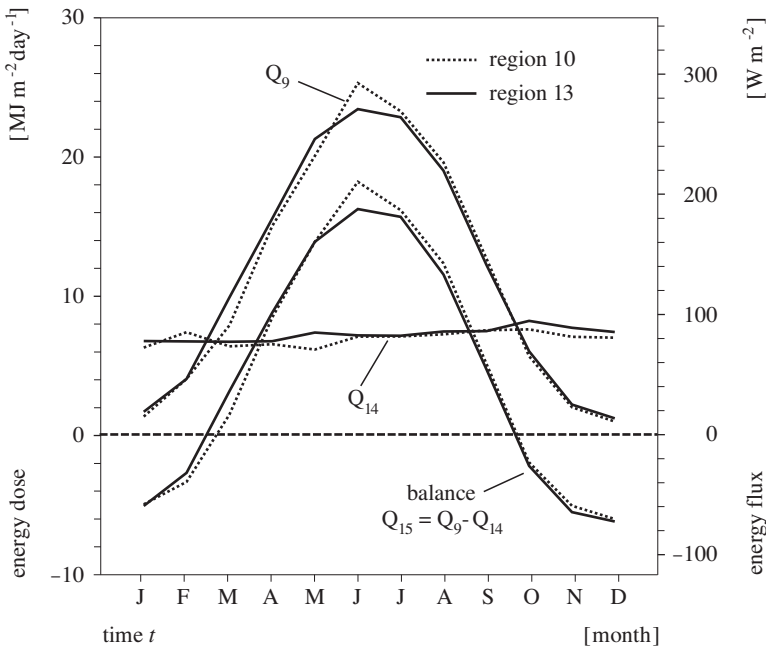


Fig. 9. Seasonal variation of solar radiation absorbed in seawater Q_9 and the effective infrared radiation at the sea surface Q_{14} for 2 selected sub-regions of the southern Baltic

months in the year is not positive throughout the year. As the examples of two sub-regions in Fig. 9 show, this varies in accordance with the seasonal changes in the energy reaching the sea surface. Values are negative in the

winter months, with a minimum diurnal mean of around $-6 \text{ MJ m}^{-2} \text{ day}^{-1}$ (-64.9 W m^{-2}) in December, whereas positive values are recorded at other times of the year, peaking at around $+17 \text{ MJ m}^{-2} \text{ day}^{-1}$ (196.8 W m^{-2}) in June. The resultant IR radiation flux across the sea surface does not change much, fluctuating around a value of $7 \text{ MJ m}^{-2} \text{ day}^{-1}$ (81 W m^{-2}). Numerous similar and other conclusions can be drawn, according to need, from the data provided in Tab. 1.

When the model was applied to southern Baltic conditions, its various elements were subjected to verification. This entailed, *inter alia*, comparison of the values computed from the model with readings obtained *in situ*. Tab. 3 exemplifies some of the results of this verification. The first two refer to the atmospheric part of the model. The diurnal values of the energy flux reaching the sea surface Q_5 , recorded on pyranometers, were compared with the corresponding values determined from the model, the input data for which were meteorological parameters measured concurrently (Fig. 10). A similar validation was carried out for hourly time intervals (item 2 in Tab. 3). The extent to which the chlorophyll *a* relationship $C_a(z) = f(C_a(0))$ predicted by the model reflects the actual chlorophyll concentration in the water column was verified using a large set of data (item 3, Tab. 3). Further, such aspects of the model as the spectral functions of light attenuation in the sea (total, or by phytoplankton pigments) $K_d(\lambda)$ and $K_{pl}(\lambda)$ were also verified. In this case for the chlorophyll concentrations measured at a given depth $C_a(z)$ the model functions $K_d(\lambda) = f(C_a(z))$ and $K_{pl}(\lambda) = f(C_a(z))$ were

Table 3. Estimated errors of the model computations

No.	Parameter	Error [%]		Number of data
		systematic	statistical	
			- +	
1	daily flux on sea surface Q_5	-5.9	14.1 14.1	22
2	irradiation – mean per hour	-4.9	43.2 43.2	375
3	total C_a in euphotic zone	-6	68 68	1400
4	$K_d(\lambda)$	4.37	19 34.4	4700
5	$K_{pl}(\lambda)$	-7.6	40.7 43.8	4600
6	K_{pl} – mean in PAR range	-6.9	36.3 36.2	578
7	absorbed energy:			
8	by water Q_{10}	-2.71	4.29 4.29	216
9	by pigments Q_{12}	5	9.02 9.02	216
10	by other admixtures Q_{11}	0.06	0.88 0.88	216
11	daily primary production Q_{13}	0.95	46.4 90.3	612

calculated and compared with the values measured *in situ* (items 4 and 5, Tab. 3). Primary production in the sea was compared with the modelled values in such a way that measurements of water temperatures, PAR just above the sea surface and surface concentrations of chlorophyll were introduced as input data in the ‘submarine’ part of the model. The modelled values of primary production computed from these data were compared with the *in situ* measurements performed by the C^{14} radioisotope method (item 11, Tab. 3). This comparison thereby verifies the entire ‘submarine’ part of the model.

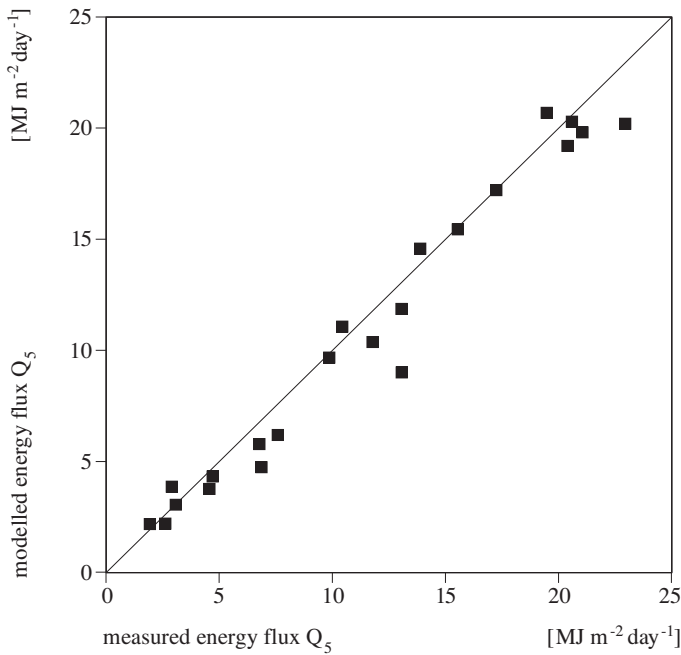


Fig. 10. Computed vs. measured values of the energy reaching the sea surface Q_5

As can be seen from Tab. 3, the magnitude of the model’s systematic errors $\langle \varepsilon \rangle$ is no greater than 10%. The statistical error in the model is understood to be the magnitude of the standard deviation σ , calculated from either linear or logarithmic statistics, *i.e.* using the expressions given below:

$$\langle \varepsilon \rangle_g = 10^{\langle \log(x_c/x_m) \rangle} - 1,$$

$$\varepsilon_{\min} = 10^{\langle \log(x_c/x_m) - \sigma_{\log} \rangle} - 1,$$

and

$$\varepsilon_{\max} = 10^{(\log(x_c/x_m) + \sigma_{\log})} - 1,$$

where

$\langle \varepsilon \rangle_g$ – geometric mean of errors,

ε_{\min} and ε_{\max} – statistical range of variability,

σ_{\log} – standard deviation of $\log(x_c/x_m)$.

The magnitudes of the errors given in Tab. 3 are due to the nature of the model employed in this work. It is a semi-empirical model, developed in such a way as to make use of mainly time- and space-averaged relationships between various optical properties of the environment and its hydrological and meteorological parameters. That is why it is not a diagnostic model enabling short-term and local values of particular energy fluxes to be calculated. On the other hand it does enable long-term, *e.g.* seasonal, aspects of the energy balance to be well determined from appropriate input data statistics.

In any case, we have to stress, that the result of calculation depends to some extent on the time averaging method (see *e.g.* Gulev, 1997). For this reason, when we apply the monthly mean meteo data set as input data to the model, the flux of energy transferred through the atmosphere (and thus the further component fluxes) may be somewhat overestimated. On the other hand, the model itself does not contain formulae for the transmission of light through high clouds; moreover, for lack of a suitable number of marine meteo data, the existing formulae for low clouds were developed in part from coastal measurements. It is therefore possible that with the present version of the model we have underestimated the quantities of energy transmitted through the atmosphere, as can be seen in item 1 of Tab. 3.

The precision of the model depends on the accuracy and the degree to which the input data are representative of a particular season and sub-region. One can thus raise the reliability of the estimated fluxes by employing satellite monitoring to obtain these data.

4. Conclusions

The result of our model computations are long-term mean values of the radiant energy fluxes in the southern Baltic region; these calculations cover all the basic radiant energy fluxes in the sea-atmosphere system. The systematic errors of the individual model computations are no more than a few percent. However, as the statistical errors of the model may be considerable, it should not be applied to computations based on a single set of short-term input data (*e.g.* for a single 24 h period) – see Tab. 3 – estimated errors of the model computations.

Of all the results obtained, the amount of energy absorbed in the sea, that re-emitted into the atmosphere by the sea surface, and the balance of these two values, are of fundamental significance for climatological research. On the other hand, the value of greatest importance for marine ecology is the energy consumed by the photosynthetic primary production of biomass in the sea.

The radiant energy balance of the southern Baltic, *i.e.* the annual mean in the entire study area, $Q_{15} = Q_9 - Q_{14}$ is clearly positive at around $1.7 \text{ GJ m}^{-2} \text{ year}^{-1}$ (53.9 W m^{-2}). This is around 20% of the solar energy reaching the atmosphere in this region. The balance Q_{15} is, however, negative in the autumn and winter months, *i.e.* from October to February, which means that at this time the sea is releasing stored energy to the atmosphere. This balance drops to a minimum, around $-6 \text{ MJ m}^{-2} \text{ day}^{-1}$ (-64.9 W m^{-2}) in December, and reaches a maximum, around $+17 \text{ MJ m}^{-2} \text{ day}^{-1}$ (196.8 W m^{-2}) in June. The effective flux of energy re-emitted by the sea surface Q_{14} does not vary significantly during the year, and fluctuates around a value of $+7 \text{ MJ m}^{-2} \text{ day}^{-1}$ (81 W m^{-2}).

The photosynthetically stored radiation Q_{13} in the water column of the southern Baltic makes up barely 0.37% of the energy absorbed by the sea throughout the year, *i.e.* about $9 \text{ MJ m}^{-2} \text{ year}^{-1}$ (the average value for the whole region). This means 0.29 W m^{-2} , or that on average around 230 g of carbon are assimilated beneath 1 m^2 of water each year.

Acknowledgements

Many thanks are due to Assoc. Professor Bogdan Woźniak and Dr. Anna Rozwadowska for their help in applying their spectral radiation transfer model.

References

- Augustyn M., 1985, *Characteristics of the southern Baltic climate*, Inst. Meteor. Water Managm., Gdynia, 61 pp.
- Bignami F., Marullo S., Santoleri R., Schiano M.E., 1995, *Longwave radiation budget in the Mediterranean Sea*, J. Geophys. Res., 100 (C2), 2501–2514.
- Bird E.R., Riordan C., 1986, *Simple solar spectral model for direct and diffuse irradiance on horizontal and tilted planes at the Earth surface for cloudless atmospheres*, Solar Energy, 25, 87–97.
- Czyszek W., Wensierski W., Dera J., 1979, *Inflow and absorption of solar energy in Baltic waters*, Stud. i Mater. Oceanol., 26, 105–140, (in Polish).
- Dera J., Rozwadowska A., 1991, *Solar radiation variability over the Baltic Sea due to weather conditions*, Oceanologia, 30, 5–36.

- Dera J., 1995, *Underwater irradiance as a factor affecting primary production*, Diss. and monogr., Inst. Oceanol. PAS, Sopot, 7, 110 pp.
- Dera J., Woźniak B., Rozwadowska A., Kaczmarek S., 1995, *Solar radiation energy absorbed by Baltic waters; the example of the Gdańsk Basins*, [in:] *First Study Conference on BALTEX, Visby, Sweden, August 28–September 1*, A. Omstedt (ed.), BALTEX Secretariat, 3, 63.
- Dobson F. W., Smith S. D., 1988, *Bulk models of solar radiation at sea*, Q. J. R. Meteor. Soc., 1145, 165–182.
- Green A. E. S., Wagner J. C., Mann A., 1988, *Analytic spectral functions for atmospheric transmittance calculations*, Appl. Opt., 27 (11), 2266–2272.
- Gulev S. K., 1997, *Climatologically significant effects of space-time averaging in the North Atlantic sea-air heat flux fields*, J. Climate, 10, 2743–2763.
- Gueymard C., 1993, *Critical analysis and performance assessment of clear sky solar irradiance models using theoretical and measured data*, Solar Energy, 51 (2), 121–138.
- ICES Rep., 1989, *Baltic Sea Patchiness Experiment PEX '86. Part 1. General Report*, Int. Council Explor. Sea, Copenhagen, 163 pp.
- Kaczmarek S., Woźniak B., 1995, *The application of the optical classification of waters in the Baltic Sea (Case 2 Waters)*, Oceanologia, 37 (2), 285–297.
- Kreżel A., 1985, *Solar radiation at the Baltic Sea surface*, Oceanologia, 21, 5–32.
- Lenoble J. 1985, *Radiative transfer in scattering and absorbing atmosphere: standard computational procedures*, A. DEEPAK Publ., Hampton, Virginia, 300 pp.
- Mobley C. D., 1994, *Light and water. Radiative transfer in natural waters*, Acad. Press, San Diego, 577 pp.
- Morel A., 1988, *Optical modelling of the upper ocean in relation to its biogenous matter content (Case 1 Waters)*, J. Geophys. Res., 93, 10749–10768.
- Morel A., 1991, *Light and marine photosynthesis: a spectral model with geochemical and climatological implications*, Progr. Oceanogr., 26, 263–306.
- Ooms M. C. (ed.), 1996, *ULISSE (Underwater Light Seatruth Satellite Experiment)*, Commiss. European Union Joint Res. Centre, Ispra, Italy, spec. publ., 1.96.29, 506 pp.
- Pomeranec K. S., 1966, *Baltic Sea heat budget*, Rep. PIHM, 1, 19–48, (in Polish).
- Raschke E., (ed.), 1996, *Radiation and water in the climate system. Remote measurements*, Springer Verlag, Berlin–Heidelberg, 617 pp.
- Timofeyev N. A., 1983, *Radiation regime of the oceans*, Nauk. Dumka, Kiyev, 247 pp, (in Russian).
- Trenberth K. E. (ed.), 1992, *Climate system modelling*, Cambridge Univ. Press, Cambridge, 788 pp.
- Woźniak B., Pelevin V. N., 1991, *Optical classification of the seas in relation to phytoplankton characteristics*, Oceanologia, 31, 25–55.

- Woźniak B., Dera J., Koblentz-Mishke O.J., 1992, *Bio-optical relationships for estimating primary production in the Ocean*, *Oceanologia*, 33, 5–38.
- Woźniak B., Rozwadowska A., 1995, *Mathematical semi-empirical model for solar radiation transmittance through the atmosphere over the South Baltic*, Inst. Oceanol. PAN Rep. 1995, 15 p., (in Polish).
- Woźniak B., Dera J., Majchrowski R., Ficek D., Koblentz-Mishke O. J., Darecki M., 1997, *'IO PAS initial model' of marine primary production for remote sensing applications*, *Oceanologia*, 39 (4), 377–395.
- Woźniak B., Rozwadowska A., Kaczmarek S., Woźniak S.B., Ostrowska M., *Seasonal variability of the solar radiation flux and its utilisation in the South Baltic*, [in:] *Proc. 21th Baltic Mar. Sci. Conf., October 22–26, 1996, Rønne, (Bornholm)*, ICES Co-operative Res. Ser., (in press).
- Woźniak S.B., 1996a, *Mathematical spectral model of solar irradiance reflectance and transmittance by a wind-ruffled sea surface. Part 1. The physical problem and mathematical apparatus*, *Oceanologia*, 38 (4), 447–467.
- Woźniak S.B., 1996b, *Sea surface slope distribution and foam coverage as functions of the mean height of wind waves*, *Oceanologia*, 38 (3), 317–332.
- Woźniak S.B., 1997, *Mathematical spectral model of solar irradiance reflectance and transmittance by a wind-ruffled sea surface. Part 2. Modelling results and application*, *Oceanologia*, 39 (1), 17–34.